

IONOSPHERIC IRREGULARITIES, SCINTILLATION AND ITS EFFECT ON SYSTEMS

Andrzej W. WERNIK¹, Lucilla ALFONSI² and Massimo MATERASSI³

¹Space Research Center, Polish Academy of Sciences
Bartycka 18a, 00-716 Warszawa, Poland
e-mail: aww@cbk.waw.pl

²Istituto Nazionale di Geofisica e Vulcanologia
Via di Vigna Murata 605, 00143 Rome, Italy

³Istituto di Fisica Applicata "Nello Carrara" (CNR)
Via Panciatichi 64, 50127 Florence, Italy

Abstract

An essential component of the ionosphere is a small-scale electron density structure that causes scintillation of radio waves on transionospheric links. We briefly review the morphology of irregularities and physical mechanisms of their formation. Results of the scintillation theory relating statistical characteristics of irregularities and scintillation are also outlined. Examples of the scintillation effect on the system performance are given. Finally, we will present recent attempts to model the scintillation.

Key words: ionospheric irregularities, ionospheric scintillation.

1. INTRODUCTION

One of the top-priority problems in the U.S. and European space weather programs is the understanding of:

– the thermosphere-ionosphere-magnetosphere interactions that control the formation and evolution of 10-km to 50-m electron density irregularities that cause scintillation,

– the relationship between those irregularities and scintillation effects on specific systems.

A high priority given to the ionospheric scintillation study comes from its significant impact on satellite radio communications. For instance, the signal distortion caused by scintillation can degrade the performance of navigation systems and generate errors in received messages. Since ionospheric scintillation originates from random electron density irregularities acting as wave scatterers, research on the formation and evolution of irregularities is closely related to scintillation studies.

Over the past four decades, there has been lively interest in this field. Many excellent reviews of scintillation theory and observations (e.g., Aarons, 1982; 1993; Yeh and Liu, 1982; Basu and Basu, 1985; 1993; Basu *et al.*, 2002; Bhattacharyya *et al.*, 1992) have been published. Comprehensive reviews of the physics of ionospheric irregularities can be found in a book by Kelley (1989) and in various papers (e.g., Keskinen and Ossakow, 1983; Kintner and Seyler, 1985; Tsunoda, 1988; Huba, 1989; Heppner *et al.*, 1993; Fejer, 1996). In this paper, we will concentrate only on selected aspects of scintillation and irregularities.

2. SCINTILLATION THEORIES

There is no doubt that scintillation of satellite radio signals is a consequence of the existence of random electron-density fluctuations within the ionosphere. These irregularities distort the original wavefront, giving rise to a randomly phase-modulated wave $k_0(\Delta\varphi)$, where for a radio wave of length λ , $k_0 = 2\pi/\lambda$ is the free-space wavenumber, and $\Delta\varphi$ is the variation of the optical path length within the layer with irregularities. $\Delta\varphi$ is dependent on the fluctuations of the ionospheric total electron content ΔN_T caused by irregularities:

$$\Delta\varphi = -2\pi r_e \Delta N_T / k_0^2, \quad (1)$$

where r_e is the classical electron radius.

As the wave propagates toward the receiver, further phase mixing occurs, changing the modulation of the wave and eventually producing a complicated diffraction pattern on the ground. If the satellite and/or the ionosphere move relative to the receiver, temporal variations of intensity and phase are recorded. Simple considerations show that the amplitude fluctuations are mainly caused by irregularities with size of the order of the first Fresnel zone $d_F = \sqrt{\lambda(z - L/2)}$, where z is the height of the upper boundary of the irregular layer, and L is the layer thickness.

This scenario of scintillation generation is valid provided $\Delta\varphi$ is not too large. If the electron density fluctuations are significant, then the phase fluctuations can be so large that the wave is no longer coherent and the interference of rays is not possible.

Analysis shows that when the phase fluctuations reach a certain limiting value, the intensity of amplitude scintillation ceases to increase.

Scintillation theory relates the observed signal statistics to the statistics of ionospheric electron density fluctuations (for reviews, refer to Yeh and Liu, 1982; Bhattacharyya *et al.*, 1992; Yeh and Wernik, 1993; Basu and Basu, 1993). The general problem of propagation of wave in a random medium is difficult to treat numerically. However, it can be greatly simplified if the wavelength is much smaller than the characteristic scale size of irregularities. In this case the wave is scattered predominantly in the forward direction and the wave propagation is described by the parabolic equation, which can be easily solved (Tatarski, 1971; Wernik *et al.*, 1980). Further simplifications are possible if the irregular layer is so thin that $\sqrt{\lambda L}$ is much smaller than the size of largest irregularity contributing to scintillation. This assumption leads to the so-called phase screen theory of scintillation in which the irregular layer is replaced by a screen, which changes only the wave's phase. The screen is located in the ionosphere at the height of the maximum electron density. Historically, the phase screen model was the first model of scintillation (Booker *et al.*, 1950; Hewish, 1951; Ratcliffe, 1956). Later expansion (Rino and Fremouw, 1977; Rino, 1980; 1982) included the geometry of propagation, anisotropy of irregularities and strong scatter case.

Knepp (1983) introduced the multiple phase screen model which let to analyze propagation of waves through a thick irregular layer with arbitrary electron density background profile.

3. IONOSPHERIC IRREGULARITIES

Both ground-based scintillation measurements and *in situ* satellite data show that ionospheric irregularities are concentrated near the magnetic equator, where they are observed in the pre-midnight period, in auroral zone during the nighttime period, and in the polar region observed at all local times. This is illustrated in Fig. 1, which is a coloured version of figure in Basu *et al.* (2002).

The main properties of the equatorial irregularities and scintillation can be summarized as follows:

- Start right after sunset when the upward drift velocity exceeds 15-20 m/s (30-45 m/s for solar maximum);
- Form plum-like structures extending occasionally above 1000 km;
- Smaller scale, field-aligned irregularities are observed within these plumes;
- Plumes are generated by the Rayleigh-Taylor instability mechanism; smaller irregularities are generated in a hierarchy of instabilities;

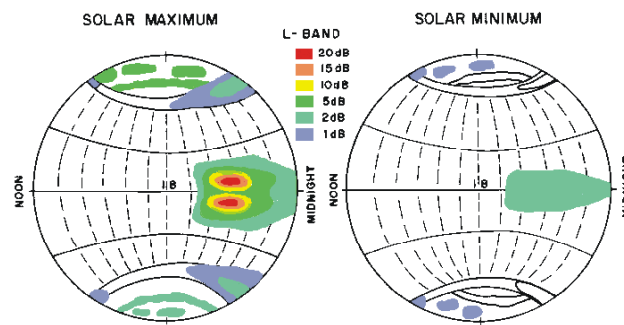


Fig. 1. Global distribution of the worst-case fading depth at L -band (coloured version of figure in Basu *et al.*, 2002).

- Scintillation is observed when the irregularity layer is sufficiently thick and is enhanced in the equatorial anomaly region where the background ionization is enhanced;
- Seasonal-longitudinal dependence of scintillation is observed (at Huancayo peaks in equinoxes and December, in Kwajalein in summer);
- Shock-like waveform is observed in the vertical direction; sinusoidal or random waveform in the horizontal direction;
- Below 300 km, $1D\ p \approx 2$ for irregularity scales of 1-10 km, and $p \approx 2.6$ for scales of 200-700 m (p is the spectral index for the irregularity spectrum);
- Above 350 km, $p \approx 1$ for kilometer scales, and $p \approx 3.2$ for meter scales.

In brief, high-latitude irregularities have the following properties:

- Scale sizes range from hundreds of kilometers down to a few centimeters and the structures are extremely dynamic, with a variable convective motion controlled by the interplanetary magnetic field (IMF);
- In the cusp and night-time auroral oval, structures at scales greater than about 50 km are created by structured fluxes of precipitating electrons;
- Under certain conditions, these structures are unstable and can produce smaller irregularities through the $\mathbf{E} \times \mathbf{B}$ or current-convective instability, wave-wave interaction and cascading;
- Large-scale structures have long lifetimes and can be convected far away from places of their origin;
- Convection is more important in the winter hemisphere;
- In summer, high E-region conductivity slows the instability growth rate and increases the cross-field plasma diffusion, effectively removing smaller-scale struc-

tures already at a short distance from the source region; consequently, smaller amplitude and larger spectral index characterize the polar-cap irregularities;

– Winter polar-cap density spectra are shallower as compared to other regions. In the winter the convecting structures decay less rapidly and are more susceptible to stirring by the velocity structure applied from the magnetosphere.

4. EFFECT OF SCINTILLATION ON SYSTEMS

As a measure of the scintillation intensity, the scintillation index S_4 is most often used. It is defined as a normalized variance of the signal power:

$$S_4^2 = \frac{\langle A^4 \rangle - \langle A^2 \rangle^2}{\langle A^2 \rangle^2}$$

If the scintillation index at a certain frequency is known, one can infer the scintillation intensity at another frequency, provided the amplitude scintillation spectral index p_s is known. Both, the theory and observations show that S_4 scales as $f_w^{-\alpha}$, where f_w is the wave frequency and $\alpha = (p_s+3)/4$. For ionospheric scintillation, the spectral index is often close to 3, and the scintillation intensity scales as $f_w^{-3/2}$. Such simple scaling is justified only for not too intense scintillation. If scintillation is moderately strong or strong, the scintillation spectrum has a form close to Gaussian and it is not possible to determine the spectral index.

Two examples of amplitude scintillation, their spectra, and cumulative probability distribution functions, corresponding to weak and moderately strong conditions, are shown in Fig. 2. Data were collected from the Hilat satellite at the Polish Polar Station on Svalbard. At high frequencies, the weak-scintillation spectrum fits quite well the power-law. However, the moderately strong scintillation spectrum appears Gaussian rather than a power-law.

In Fig. 2 we also show the experimental cumulative probability-density function and the best-fit log-normal density function. While, for weak scintillation, the experimental and theoretical probabilities agree satisfactorily, for strong scintillation they differ markedly. Fremouw *et al.* (1980) have made a thorough analysis of scintillation statistics. They concluded that the best fit to the observed amplitude and phase scintillation is obtained with a two-component model. In this model, it is postulated that the high-frequency, diffractively scattered component obeys generalized Gaussian statistics and the low-frequency, refractively focused component obeys log-normal statistics. Wernik (1997), who applied wavelet filtering to investigate the probability distribution function of scintillation at selected frequencies, later confirmed this conclusion. Phase is nearly always normally distributed, without regard to the strength of scatter.

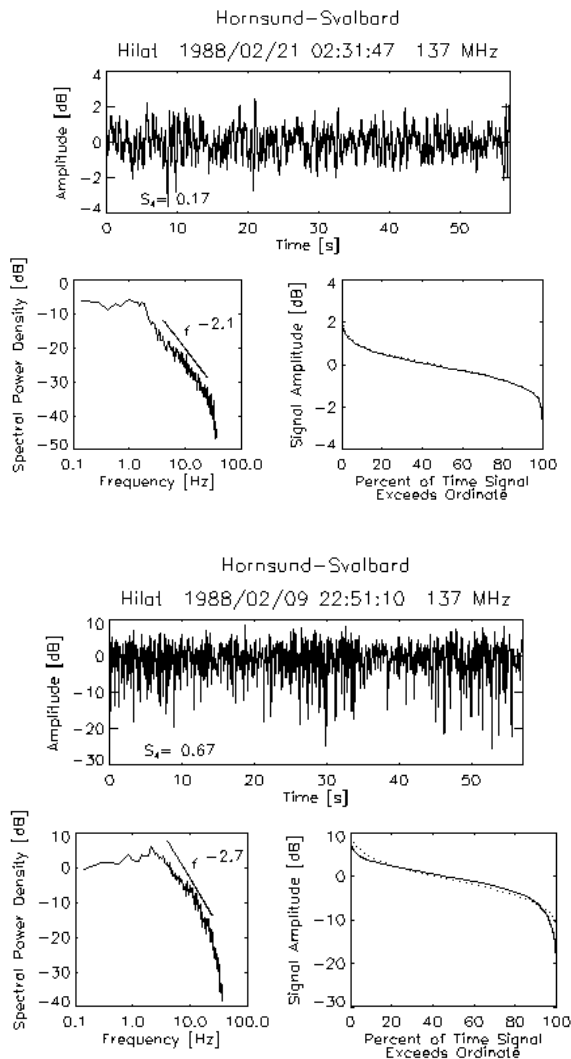


Fig. 2. Examples of the amplitude scintillation, their power spectra and cumulative probability densities for weak (upper frames) and moderately strong (lower frames) scintillation. The power-law fit to each spectrum between 4 and 25 Hz is shown. The dotted line is the log-normal probability density (Wernik *et al.*, 2003).

The main effect of scintillation on the transionospheric radio systems is the signal loss and cycle slips, causing difficulties in the lock of receivers to a signal. This effect is especially dangerous when scintillation is strong.

Knepp (1983) has simulated the effect of scintillation on the pulse shape and delay. We have repeated his simulations using more realistic model of the ionosphere. An example is shown in Fig. 3. One can see that even for moderate scintillation activity, the instantaneous excess time delay may reach 2 ns, or 20% of the excess time due to the background ionization. This corresponds to 0.6 m in range error. Apparently,

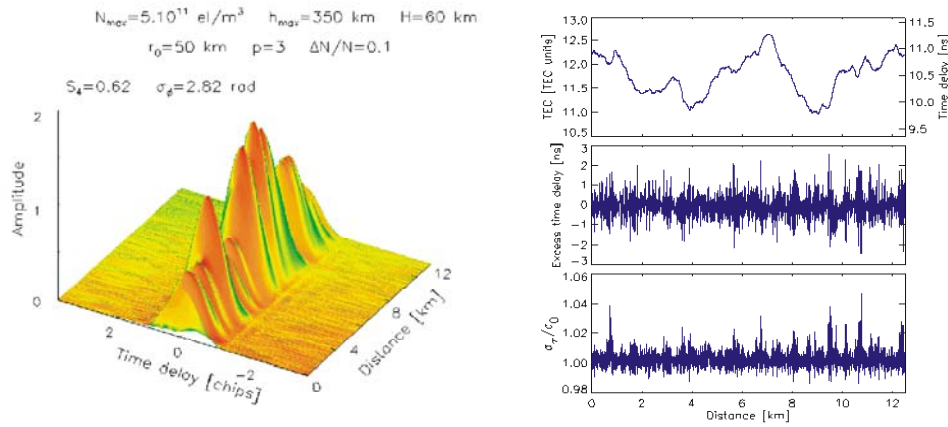


Fig. 3. The GPS pulse distortion due to random irregularities (left). The Chapman electron density profile is assumed. Parameters of the profile and of the irregular ionosphere are shown. Multiple phase screen model was used in the calculations. Vertical incidence is assumed. Distance is a distance along the satellite trajectory on the ground. The TEC (total electron content) variations is shown at the top panel of the right figure. The excess time delay is a delay in excess of that caused by regular TEC variations. The bottom panel shows the pulse spread relative to the undisturbed spread.

time averaging greatly reduces the pulse distortion effects. Yeh and Liu (1979) investigated statistics and the temporal moments of pulses in the random media with application to the ionosphere.

5. MODELLING OF SCINTILLATION

In local modelling of scintillation, based on either the multiple phase screens or parabolic equation, the following parameters have to be taken into account:

- background electron density profile $N(h)$ (in a single phase screen model maximum electron density N_{max} , height of the maximum h_{max} , height of the phase screen h , irregularity slab thickness L);
- irregularity amplitude profile $\Delta N/N$ (in a single phase screen model variance of the irregularity amplitude);
- 3D spectral index of irregularity spectrum p (*in situ* measurements give 1D spectral index $p_1 = p - 2$, phase and amplitude spectral index $p_s = p - 1$);
- outer scale of turbulence r_0 ,

- elongation α of irregularities along magnetic field \mathbf{B} ,
- elongation β transverse to \mathbf{B} ,
- inclination δ of transverse irregularity axis,
- magnetic dip I at the observation site.

Figure 4 shows the results of modelling of the distribution of scintillation index S_4 and phase variance σ_ϕ using a single phase screen. Calculations followed the derivations by Rino and Fremouw (1977).

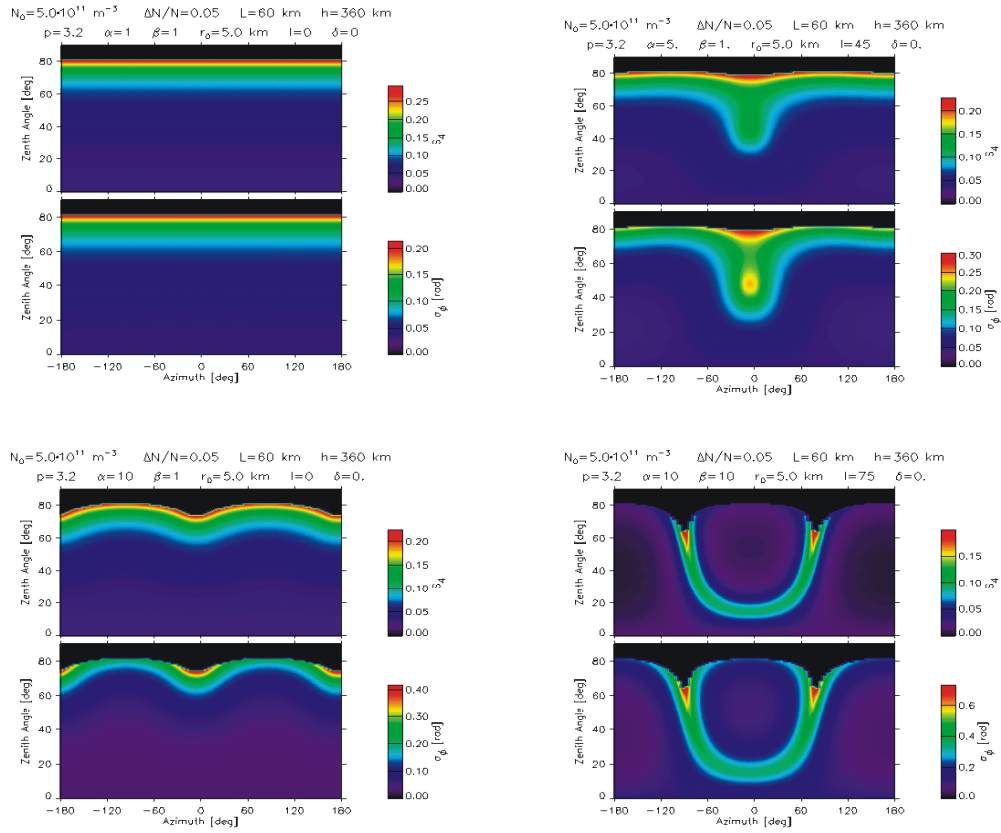


Fig. 4. Distribution of the scintillation index S_4 and phase variance σ_ϕ over the sky at various locations specified by the dip angle I . Azimuth is the magnetic azimuth. The wave frequency is 1200 MHz. The upper left panel corresponds to isotropic irregularities. The upper right panel represents a typical mid-latitude situation. The lower left panel simulates the scintillation at the equator with highly elongated irregularities. The lower right panel shows the distribution of scintillation at high latitudes for sheet-like irregularities with respect to the magnetic L shell. The areas where the weak scatter approximation breaks down are in black.

6. GLOBAL MODELS OF SCINTILLATION

The WBMOD ionospheric scintillation model (Fremouw and Secan, 1984; Secan *et al.*, 1995) and its upgrades (SCINTMOD) (Secan *et al.*, 1997) contain the worldwide climatology of the ionospheric plasma-density irregularities that cause scintillation (environment model), coupled to a model for the effects of these irregularities on a transionospheric radio signals (propagation model). The propagation model is a phase-screen model (Rino, 1979) in which the ionospheric irregularities are characterized by a power-law power-density spectrum.

The model for the propagation effects is based on a three-dimensional description of the plasma density irregularities with the following parametrization: axial ratio of the irregularities along and across the local magnetic field direction; the orientation of sheet-like irregularities with respect to the magnetic L shells; the logarithmic slope and outer scale of the *in situ* spatial spectrum of the irregularities; the height-integrated strength of the spatial spectrum, defined at a scale size of 1 km ($C_k L$); the height of the phase screen; and the *in situ* velocity of irregularities. WBMOD includes models for each of these parameters, some derived from analysis of scintillation data, and others (the *in situ* drift velocity, for example) based on analysis of a variety of other data sets.

For a discussion of limitations of WBMOD the reader might wish to consult a review by Wernik *et al.* (2003). Here we just point out that WBMOD is a global climatological model and, as such, is unable to describe the extreme day-to-day variability of scintillation, being useful only for a long-term forecasting.

Recently, a model based on the *in situ* satellite data has been proposed (Alfonsi *et al.*, 2003). It makes use of a large bank of *in situ* plasma density data collected by the Dynamics Explorer-B satellite to derive scintillation parameters. From the density N measured at the satellite height the relative density fluctuations $\Delta N/N_0 = (N - N_0)/N_0$ are calculated, where N_0 is the smooth background density. Assuming that $\Delta N/N_0$ does not change with height, ΔN at the peak of F-layer is calculated using the density profile derived from the ionosphere model, for instance IRI (International Reference Ionosphere). Scintillation along the projection of the satellite orbit on the ground (x coordinate) is simulated using the Fresnel-Kirchhoff formulation of the phase screen theory for wave propagation through the random ionosphere (Yeh and Liu, 1982)

$$u(x, z) \equiv A(x, z) \exp[i\phi(x, z)] = A_0 \sqrt{\frac{ik}{2\pi z}} \iint \exp\left\{-i\left[\Delta\varphi(x') + \frac{k}{2z}|x-x'|^2\right]\right\} dx', \quad (2)$$

where A_0 is the amplitude of incident wave, z is the effective height of the phase screen, $\Delta\varphi$ are the phase variations on the screen, as given by formula (1).

We assume that the phase screen is located at the effective height defined as

$$h_{\text{eff}} = \int_0^{h_s} h N_0(h) dh \bigg/ \int_0^{h_s} N_0(h) dh,$$

where h_s is a certain height well above the F-layer peak height. In our modelling we assumed $h_s = 1000$ km.

The irregularity slab thickness L , needed to estimate $\Delta N_T \approx \Delta N \cdot L$, is calculated as a distance between points on the profile $N_0(h)$ at which the density falls to a predefined fraction of its maximum value.

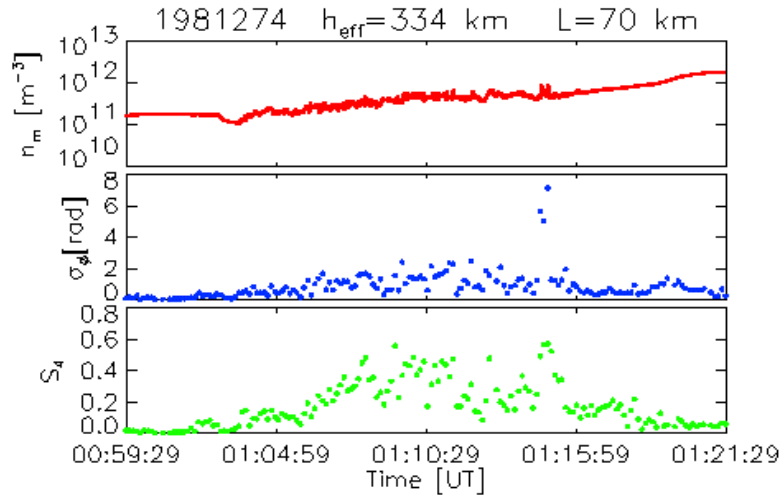


Fig. 5. Example of scintillation simulations. The top panel shows the electron density variations along the satellite orbit and rescaled to the F-layer peak density. Next two panels show the rms phase σ_ϕ and scintillation index S_4 .

Figure 5 shows an example of scintillation simulations at 1200 MHz for an arbitrarily chosen satellite path. Simulations performed for a large number of satellite orbits allow covering large area of the globe with scintillation ‘measurements’ and produce maps of scintillation parameters. Such maps can be sorted in dependence on the geophysical conditions, such as season, time, K_p magnetic index, any solar activity index, orientation of the interplanetary magnetic field etc., for a later use in the prediction of scintillation activity at a given satellite-receiver link.

Neither WBMOD nor the proposed model of scintillation allows short-term forecasts of scintillation. Such forecasts, albeit presently limited to the American sector of equatorial region, offers SCINDA (**Scintillation Network Decision Aid**) (Groves *et al.*, 1997). SCINDA makes use of scintillation data from available satellite links and ionospheric drift velocities measured and stored at the remote sites. At fifteen-minute intervals, this information is retrieved and combined with the empirical model of equatorial bubble dynamics to make simple tri-color maps of disturbances over the equator and the corresponding areas of likely communication outages.

7. CONCLUSIONS

In conclusion we point out some outstanding problems pertinent to the scintillation modelling and forecasting of scintillation effects on satellite based communication and navigation systems.

- The scintillation theory is well developed, but simple algorithms of use in the scintillation modelling should be worked out.
- The effect of scintillation on systems (e.g., ranging, navigation) should be further studied.
- The existing (e.g., WBMOD) can be improved by enlarging the scintillation data set from a network of stations, e.g., GPS.
- Models useful in predicting the day-to-day and short term, as magnetic storm, variability of scintillation should be constructed.
- *In situ* satellite data can be used in the future scintillation models.
- Attempts should be made to develop the physics-based models of scintillation.
- Satellite *in situ* measurements of plasma density, electric and magnetic fields, plasma velocity, particle flux etc. would help in nearly real-time forecasting of scintillation.

References

- Aarons, J., 1982, *Global morphology of ionospheric scintillation*, Proc. IEEE **70**, 360-378.
- Aarons, J., 1993, *The longitudinal morphology of equatorial F-layer irregularities relevant to their occurrence*, Space Sci. Rev. **63**, 209-243.
- Alfonsi, L., M. Materassi and A.W. Wernik, 2003, *Distribution of scintillation parameters calculated from in situ data – preliminary results*, Proceedings of “Atmospheric Remote Sensing using Satellite Navigation Systems”, Special Symposium of the URSI Joint Working Group FG, Matera, October 2003.
- Basu, S., and S. Basu, 1985, *Equatorial scintillations: Advances since ISEA-6*, J. Atmos. Terr. Phys. **47**, 753-768.
- Basu, S., and S. Basu, 1993, *Ionospheric structures and scintillation spectra*. In: V.I. Tatarski, A. Ishimaru and V.U. Zavorotny (eds.), “Wave Propagation in Random Media (Scintillation)”, pp. 139-153, The International Society for Optical Engineering, Bellingham, WA, USA.
- Basu, S., K.M. Groves, Su. Basu and P.J. Sultan, 2002, *Specification and forecasting of scintillations in communication/navigation links: current status and future plans*, J. Atmos. Solar-Terr. Phys. **64**, 1745-1754.

- Bhattacharyya, A., K.C. Yeh and S.J. Franke, 1992, *Deducting turbulence parameters from transiono-spheric scintillation measurements*, Space Sci. Rev. **61**, 335-386.
- Booker, H.G., J.A. Ratcliffe and D.H. Shinn, 1950, *Diffraction from an irregular screen with application to ionospheric problems*, Phil. Trans. Roy. Soc. A. **242**, 579.
- Fejer, B.G., 1996, *Natural ionospheric plasma waves*. In: H. Kohl, R. Rüster and K. Schlegel (eds.), "Modern Ionospheric Science", pp. 216-273, European Geophysical Society, Katlenburg-Lindau, FRG.
- Fremouw, E.J., and J.A. Secan, 1984, *Modelling and scientific application of scintillation results*, Radio Sci. **19**, 687-694.
- Fremouw, E.J., R.C. Livingston and D.A. Miller, 1980, *On statistics of scintillating signals*, J. Atmos. Terr. Phys. **42**, 717-731.
- Groves, K.M., S. Basu, E.J. Weber, M. Smitham, H. Kuenzler, C.E. Valladares, R. Sheehan, E. Mackenzie, J.A. Secan, P. Ning, W.J. McNeill, D.W. Moonan and M.J. Kendra, 1997, *Equatorial scintillation and systems support*, Radio Sci. **32**, 2047-2064.
- Heppner, J.P., M.C. Liebrecht, N.C. Maynard and R. F. Pfaff, 1993, *High-latitude distributions of plasma waves and spatial irregularities from DE 2 alternating current electric field observations*, J. Geophys. Res. **98**, 1629-1652.
- Hewish, A., 1951, *The diffraction of radio waves in passing through a phase-changing ionosphere*, Proc. Roy. Soc. A. **209**, 81.
- Huba, J.D., 1989, *Theoretical and simulation methods applied to high latitude, F region turbulence*. In: C.H. Liu (ed.), "World Ionosphere/Thermosphere Study", WITS Handbook, vol. 2, pp. 399-428, SCOSTEP Secretariat, Boulder, CO.
- Kelley, M.C., 1989, *The Earth Ionosphere*, Academic Press, London.
- Keskinen, M.J., and S.L. Ossakow, 1983, *Theories of high-latitude irregularities: A review*, Radio Sci. **18**, 1077-1092.
- Kintner, P.M., and C.E. Seyler, 1985, *The status of observations and theory of high latitude ionospheric and magnetospheric plasma turbulence*, Space Sci. Rev. **41**, 91-129.
- Knepp, D. L., 1983, *Multiple phase-screen calculation of the temporal behavior of stochastic waves*, Proc. IEEE **71**, 722-737.
- Ratcliffe, J.A., 1956, *Some aspects of diffraction theory and their application to the ionosphere*, Rep. Progr. Phys. **19**, 188-267.
- Rino, C.L., 1979, *A power law phase screen model for ionospheric scintillation, 2, Strong scatter*, Radio Sci. **14**, 1147-1155.
- Rino, C.L., 1980, *Numerical computations for a one-dimensional power law phase screen*, Radio Sci. **15**, 41-47.
- Rino, C.L., 1982, *On the application of phase screen models to the interpretation of ionospheric scintillation data*, Radio Sci. **17**, 855-867.
- Rino, C.L., and E.J. Fremouw, 1977, *The angle dependence of singly scattered wavefields*, J. Atmos. Terr. Phys. **39**, 859-868.

- Secan, J.R., R.M. Bussey, E.J. Fremouw and S. Basu, 1995, *An improved model of equatorial scintillation*, Radio Sci. **30**, 607-617.
- Secan, J.R., R.M. Bussey and E.J. Fremouw, 1997, *High-latitude upgrade to the Wideband ionospheric scintillation model*, Radio Sci. **32**, 1567-1574.
- Tatarski, V.I., 1971, *The effects of the turbulent atmosphere on wave propagation*, Natl. Tech. Inform. Serv., Springfield, VA.
- Tsunoda, R.T., 1988, *High latitude F region irregularities: A review and synthesis*, Rev. Geophys. Space Phys. **26**, 719-760.
- Wernik, A.W., C.H. Liu and K.C. Yeh, 1980, *Model computation of radio wave scintillation caused by equatorial ionospheric bubbles*, Radio Sci. **15**, 559-572.
- Wernik, A.W., 1997, *Wavelet transform of nonstationary ionospheric scintillation*, Acta Geophys. Pol. **45**, 237-253.
- Wernik, A.W., J.A. Secan and E.J. Fremouw, 2003, *Ionospheric irregularities and scintillation*, Adv. Space Res. **31**, 4, 971-981.
- Yeh, K.C., and C.H. Liu, 1979, *Ionospheric effects on radio communication and ranging pulses*, IEEE Trans. Antennas and Prop. **AP-27**, 747-751.
- Yeh, K.C., and C.H. Liu, 1982, *Radio wave scintillations in the ionosphere*, Proc. IEEE **70**, 324-360.
- Yeh, K.C., and A.W. Wernik, 1993, *On ionospheric scintillation*. In: V.I. Tatarski, A. Ishimaru and V.U. Zavorotny (eds.), "Wave Propagation in Random Media (Scintillation)", pp. 34-49, The International Society for Optical Engineering, Bellingham, WA, USA.

Received 21 January 2004
Accepted 28 January 2004